Fermi National Accelerator Laboratory

FERMILAB-Pub-76/77-THY
September 1976

Many-Body Scattering Processes in a One-Dimensional Boson System

H. B. THACKER
Fermi National Accelerator Laboratory, Batavia, Illinois 60510

ABSTRACT

The one-dimensional many-body problem described by the non-relativistic $|\phi|^4$ theory of a complex scalar boson field (also known as the δ-function model) is studied. By induction, it is shown that the set of nth order perturbation theory graphs for the N-particle in-state wave function can be combined and reduced to an equivalent set of factorized graphs in which the particle lines are numbered according to their ordering in momentum space at time $t = -\infty$. By carrying out loop integrations, each factorized graph is reduced to one of a finite number of skeleton graphs multiplied by a dressing function. The dressing functions are related to the multiparticle phase shifts which appear in Bethe's form of the N-body wave function. The skeleton graphs are shown to be associated with the ordering of particles in configuration space which characterizes Bethe's hypothesis. The analogy of a classical system of billiard balls is found to be helpful in interpreting the form of Bethe's hypothesis and the physical significance of the skeleton graphs. The use of factorized graphs in the scattering theory of statistical mechanics is demonstrated by a graphical calculation of the second virial coefficient.

Operated by Universities Research Association Inc. under contract with the Energy Research and Development Administration

I. INTRODUCTION

This is the second in a series of papers[1] dealing with the many-body problem in one space dimension described by the Hamiltonian

$$H = \int dx\left\{[\nabla \phi^*(x)][\nabla\phi(x)] + c\,\phi^*(x)\phi^*(x)\phi(x)\phi(x)\right\} \tag{1.1}$$

where $\phi(x)$ is a quantized boson field and c is a coupling constant. This Hamiltonian corresponds to a local Lagrangian density

$$\mathscr{L} = \frac{i}{2}\phi^*\overleftrightarrow{\partial}_0\phi - (\nabla\phi^*)(\nabla\phi) - c\phi^*\phi^*\phi\phi. \tag{1.2}$$

This model has been discussed previously by a number of authors[2-7] and has proven to be surprisingly amenable to exact analysis. However, these discussions have all been in the context of the first-quantized formalism, in which an N-particle system is described by an N-body wave function which is an eigenfunction of the operator

$$H = -\sum_{i=1}^{N}\frac{\partial^2}{\partial x_i^2} + 2c\sum_{i<j\le N}\delta(x_i - x_j)\ . \tag{1.3}$$

The advantage of this formulation is that it allows one to invoke Bethe's hypothesis,[8] which provides a complete set of eigenfunctions of (1.3). All previous discussions of this model use Bethe's wave functions as a starting point. On the other hand, all the N-body problems (N = 1, 2, 3, ...) defined by (1.3) can be subsumed under the quantum field theory (1.1)

or (1.2).[9] In view of the fact that modern many-body theory is largely built around the field theoretic formulation of the many-body problem, it seemed desirable to investigate the behavior of this model from a different point of view in which (1.1) or (1.2) served as the starting point. From this point of view, we would expect Bethe's wave functions, as well as other known results (e.g. the S-matrix[2] and the equation of state[6]), to emerge from the appropriate field theoretic calculation. In addition to providing a clearer understanding of known results, such an approach may yield calculational tools which would allow us to consider other properties of finite density systems which have not yielded to the Bethe's hypothesis approach.

Motivated by these and related considerations, we began some time ago an investigation[1] of the properties of multiparticle systems described by (1.1) or (1.2), using the standard graphical techniques of quantum field theory. Roughly speaking, we can divide the properties to be investigated into two categories, those relating to zero density systems (scattering theory) and those relating to finite density systems (statistical mechanics). The first interesting problems in the scattering theory of this model are encountered in the three-body system. The Feynman graph combinatorics of the three-body scattering problem were resolved in I. In this paper, we complete the investigation of scattering theory by explicitly summing all terms in the graphical expansion of the in-state wave function for any number of particles N. This is accomplished by decomposing and rearranging the set of Feynman graphs in each order of perturbation theory to produce

a new set of "factorized" graphs. By an induction on the order of perturbation theory, the evolution from Feynman graphs to factorized graphs is demonstrated to all orders. The calculation and topological classification of the factorized graphs is much simpler than that of the corresponding Feynman graphs. It is found that the performance of a loop integration on a factorized graph is equivalent to removing an internal line from the graph and multiplying the resulting graph by a factor which depends on the initial state momenta (but not on any of the remaining loop momenta). In this way, any multi-loop graph can be reduced to one of a finite number of relatively simple graphs (which will be referred to as the skeleton of the multi-loop graph) multiplied by a certain function of the initial momenta. The graphical expansion of an in-state wave function can thus be written in terms of a finite number of skeletons, each one multiplied by a "dressing" function which is an infinite series in the coupling constant. The dressing of each skeleton is a function of the variables k_i, $i = 1, \ldots, N$, the momenta of the N-particle plane wave state $|k\rangle$ from which the in-state $|\Psi^{(+)}(k)\rangle = U(0, -\infty)|k\rangle$ evolves (here, $U(t, t') = e^{iH_0 t} e^{iH(t' - t)} e^{-iH_0 t'}$ is the time development operator in the interaction picture). The dressing functions are related to the phase shift factors which appear in Bethe's wave functions. The analytic properties of the momentum space wave function $\langle p|\Psi^{(+)}(k)\rangle$ in the N momentum variables p_i reside entirely in the skeleton graphs themselves, which can be associated with the configuration space ordering which characterizes Bethe's hypothesis.

In Section II the rules for factorized graphs are stated and a topological classification scheme is introduced. The separation of a factorized graph into (skeleton) × (dressing function) is described and equivalence to ordinary perturbation theory is established for the two-body system. In Section III the general procedure is described by which the perturbation series for the N-body wave function reduces to a set of factorized graphs to each order in c for any number of particles N. The formalism thus developed is applied in Section IV to a detailed investigation of the many-body wave functions, and the connection between the skeleton expansion and Bethe's hypothesis is traced. An analogy to a system of classical billiard balls moving in one dimension is found to be very helpful in understanding the nature of Bethe's hypothesis and the physical significance of the skeleton expansion. Some initial efforts toward an extension of these techniques to finite density systems are described in Section V. Using a technique related to that of Goldberger,[10] and Dashen, Ma, and Bernstein,[11] the second virial coefficient is expressed in the language of operator scattering theory and calculated via factorized graphs. It is noted that the momentum derivative acting on the phase shift in the two-body density of states can be interpreted as the manifestation of a forward singularity of a matrix element.

II. FACTORIZED GRAPHS, SKELETONS, AND TWO-BODY SCATTERING

The understanding of multiparticle scattering which will be developed in Sections III and IV relies heavily on a graphical representation of the many-body in-state wave function in each order of perturbation theory. In this section we introduce the basic elements of these graphs (which will be referred to as "factorized" graphs) and discuss some of their properties.

The N-body in-state wave function can be constructed from a free N-particle plane wave state $|k_1 k_2 \ldots k_n\rangle \equiv |k\rangle$ by a perturbative expansion of the Lippmann-Schwinger equation,

$$|\Psi^{(+)}(k)\rangle = \sum_{n=0}^{\infty} \left[G_0(\omega_k)V\right]^n |k\rangle, \tag{2.1}$$

where G_0 is the free particle Green's function operator

$$G_0(\omega) = \frac{1}{\omega - H_0 + ie} , \tag{2.2}$$

H_0 and V are the first and second terms in (1.1) respectively, and ω_k is the energy of the plane wave

$$\omega_k = \sum_{i=1}^{N} k_i^2 . \tag{2.3}$$

The mass of the particles has been set equal to 1/2 for convenience. The momentum space wave function $\langle p|\Psi^{(+)}(k)\rangle$ can, by virtue of (2.1), be

calculated by a set of graphs in each order of perturbation theory, representing vertices, energy denominators, and loop integrations. These will be referred to as ordinary perturbation theory graphs. We will also have occasion to consider graphs which are obtained from matrix elements of the form $\langle p \left| V\left[G_0(\omega_k)V\right]^n \right| k\rangle$ which will be called amplitude graphs. The latter can also be obtained by carrying out all energy integrations on the corresponding Feynman graphs (see I for further discussion). The basic vertex

$$\langle p_1 p_2 \left| V \right| q_1 q_2 \rangle = 4c(2\pi)\delta(p_1 + p_2 - k_1 - k_2) \tag{2.4}$$

will be represented by a dotted interaction line connecting two particle lines, Fig. 1. This is a change in graphical notation from I, where (2.4) was represented by a single 4-point vertex. The convenience of the present notation will become apparent. It will be important to keep in mind that, in spite of appearances, Fig. 1 contains no dependence on the momentum exchanged across the interaction line and is symmetric under the interchange $p_1 \leftrightarrow p_2$. Throughout this paper, the letter k will be reserved for the momentum variables of the plane wave from which the in-state is constructed, and the argument of G_0, unless otherwise indicated, is understood to be ω_k. In constructing the in-state $\left| \Psi^{(+)}(k) \right\rangle$ by successive applications of V and G_0, the k's never appear as integration variables, which allows us to choose a particular ordering, viz.

$$k_1 < k_2 < \ldots < k_N \quad . \tag{2.5}$$

Now let us define the basic element of a factorized graph, the wiggly, directed exchange line shown in Fig. 2. In an N-body factorized graph, there are N particle lines proceeding from the initial momenta k_i at the bottom of the graph to the final momenta p_i at the top. Each line is numbered from 1 to N according to the ordering of the momentum it carries in the initial state, e.g. for the ordering (2.5), the line carrying momentum k_ℓ would be numbered ℓ. Graphs will always be symmetrized over the final momenta p_i corresponding to the Bose symmetry of the wave function. A factorized graph of nth order in the coupling constant will have n exchange lines like that shown in Fig. 2, each of which connects a pair of numbered particle lines. The direction of the exchange line is always from the lesser numbered line to the greater numbered line. The value of a factorized graph is given by the following rules:

(a) A momentum pole

$$\frac{-i}{q - i\epsilon}$$

for an exchange line of momentum q. (2.5a)

(b) A line dependent "coupling constant"

$$x_{ij} = \frac{ic}{k_i - k_j}$$

for each exchange line connecting numbered particle lines i and j, $i < j$. (2.5b)

(c) An integration $\int \frac{dq}{2\pi}$ for each closed loop. (2.5c)

(d) A factor of two for each distinct pair of numbered particle lines which is connected by one or more exchange lines. (2.5d)

The properties of factorized graphs will become clearer in the subsequent discussion of multiparticle scattering, but at this point it is worth emphasizing some of their structural properties which can be inferred directly from the rules (2.5). First of all, instead of merely specifying the order n of a graph in the coupling constant, where n is the total number of interaction vertices in the graph, a factorized N-particle graph can be characterized by a set of $N(N-1)/2$ numbers $\{n_{ij}\}$, $i < j \leq N$, where n_{ij} is the number of exchanges between the particle lines numbered i and j. The order of the graph is then

$$n = \sum_{i<j\leq N} n_{ij} \quad . \tag{2.6}$$

The set of numbers $\{n_{ij}\}$ will be called the topological index or simply the topology of the graph. This notation will sometimes be abbreviated, viz. $\{n_{ij}\} \rightarrow \{n\}$. When explicitly writing the topological index of a graph, we will arrange the numbers n_{ij} such that all numbers n_{1j} are first, in order of increasing j, then all numbers n_{2j}, and so forth. Thus, the index of the 4-particle graph in Fig. 3(a) is $\{3, 1, 0, 0, 2, 2\}$.

Next we note that the value of a factorized wave function graph for given initial and final momenta is independent of the time-ordering of the

exchange lines and is in fact completely specified by the topological index $\{n_{ij}\}$. (Moreover, it will be found that, in the construction of the many-body wave function, graphs with the same index and different orderings should be considered identical and counted only once.) The fact that the time ordering of the exchange lines can be permuted without changing the value of the graph is a key property which allows us to push together all exchange lines which connect a particular pair of particle lines. For example, the graph shown in Fig. 3(a) is equivalent to the graph in Fig. 3(b).

Since the value of a factorized graph is entirely specified by its topological index $\{n\}$, we will use $\mathcal{G}(\{n\})$ to denote a particular graph. It will now be shown that a factorized graph $\mathcal{G}(\{n\})$ can be written as a product of two factors

$$\mathcal{G}(\{n\}) = \mathcal{D}(\{n\})\mathcal{K}(\{n\}) \quad . \tag{2.7}$$

The first quantity $\mathcal{D}(\{n\})$ will be called the dressing function of the graph and contains all the factors of x_{ij} which arise from rule (2.5b), as well as all the numerical factors from rule (2.5d). The second quantity $\mathcal{K}(\{n\})$ is the skeleton of the graph, and is obtained by ignoring all factors arising from rules (2.5b) and (2.5d) and computing the graph by rules (2.5a) and (2.5c) only. It will be convenient to define a set of numbers $\{\hat{n}_{ij}\}$ associated with each set $\{n_{ij}\}$, where

$$\hat{n}_{ij} = 0 \quad \text{if } n_{ij} = 0 \tag{2.8a}$$

$$\hat{n}_{ij} = 1 \quad \text{if } n_{ij} \neq 0 \quad . \tag{2.8b}$$

The skeleton of a graph can, in general, be greatly simplified by a few graphical operations which correspond to carrying out most of the loop integrations. First, the commutability of the vertices can be used to bunch together all the exchange lines connecting a particular pair of particle lines, as we did, for example, in going from Fig. 3(a) to Fig. 3(b). Then the identity shown in Fig. 4,

$$\int \frac{dq}{2\pi} \left(\frac{-i}{q - i\epsilon}\right)\left(\frac{-i}{q' - q - i\epsilon}\right) = \frac{-i}{q' - i\epsilon} \tag{2.9}$$

can be used to remove all but one of the exchange lines connecting that pair. The skeleton of Fig. 3(a) thus reduces to Fig. 3(c). In general, this procedure gives us the skeletal identity

$$\mathscr{K}(\{n\}) = \mathscr{K}(\{\hat{n}\}) \quad . \tag{2.10}$$

From rules (2.5b) and (2.5d), the dressing function of an arbitrary graph $\mathscr{G}\{n\}$ can be written explicitly in terms of its topological index,

$$\mathscr{D}(\{n\}) = 2^{\hat{n}} \left\{ \prod_{i<j\leq N} (x_{ij})^{n_{ij}} \right\} \tag{2.11}$$

where $\hat{n}$ is the number of exchange lines in the skeleton after it has been reduced by (2.10), i.e.,

$$\hat{n} = \sum_{i<j\leq N} \hat{n}_{ij} \quad . \tag{2.12}$$

The first factor in (2.11) is dictated by rule (2.5d) and the second by rule (2.5b). Eqns. (2.10) and (2.11) will be extremely useful, both in the reduction of ordinary perturbation theory graphs to factorized graphs and in the summing up of factorized graphs to calculate the many-body wave function.

In the next section we will give the explicit inductive procedure by which the ordinary nth order perturbation theory graphs for the N-body wave function, for any number of particles N, reduce to an equivalent set of nth order factorized graphs. Although the utility of the factorized graphs becomes fully apparent only at the level of the N-body problem, $N \geq 3$, a brief consideration of two-body scattering is instructive. Because of the simplicity of the two-body system, the factorized graphs offer no great calculational advantage over ordinary perturbation theory, and the present discussion, which may seem unnecessarily complicated, is designed with the N-body problem in mind. By virtue of (2.1), the construction of the (n + 1)th order wave function graphs can be viewed as a two-step operation on the nth order wave function graphs. First the operator V is applied to the nth order part of the state $|\Psi^{(+)}(k)>$. Graphically, this contracts together a pair of lines at the top of the graph into a vertex like (2.4), converting the nth order wave function graph into an (n + 1)th order amplitude graph. The total result of applying V to an N-particle wave

function graph is the sum of the $N(N-1)/2$ possible contractions. All the particles are then propagated forward in time by the energy denominator arising from the action of G_0 on the $(n+1)$th order amplitude graph, yielding an $(n+1)$th order wave function graph. To zeroth order in the coupling constant, the equivalence of ordinary and factorized graphs is trivial. We therefore assume that the nth order wave function graphs have been combined and factorized and demonstrate the construction and factorization of the $(n+1)$th order graphs.

For two-body scattering, there is only one factorized wave function graph in each order of perturbation theory, e.g. Fig. 5(a) for $n = 3$. Its topological index is a single number $n_{12} = n$ = order of the graph. By rules (2.5b and d) the dressing function is

$$\mathscr{D}(\{0\}) = 1 \tag{2.13a}$$

$$\mathscr{D}(\{n\}) = 2x_{12}^{n}, \quad n \neq 0 \quad . \tag{2.13b}$$

Because of (2.10) and (2.8), there are only two distinct skeletons, the non-interacting graph (summed over the orderings of final state momenta),

$$\mathscr{G}(\{0\}, p) = 2\,\mathscr{S}_p(2\pi)\delta(p_1 - k_1) \tag{2.14a}$$

and the one-exchange skeleton, Fig. 5(b),

$$\mathscr{G}(\{1\}, p) = 2\,\mathscr{S}_p\left(\frac{-i}{k_1 - p_1 - i\epsilon}\right). \tag{2.14b}$$

The momentum space wave function $\langle p \mid \Psi^{(+)}(k)\rangle$ is given by the sum of graphs multiplied by (2π) times an overall momentum conserving δ-function. The symbol $\mathscr{S}$ in (2.14) is defined in Eq. (6) of I. It indicates a symmetrization over the momentum variables of a particular state. When the momentum dependence of a graph is indicated explicitly, as in (2.14), the variables exhibited will always be the momenta of the final state particles. The application of V to the nth order two-body wave function graph gives the $(n+1)$th order amplitude graph, e.g. Fig. 5(c) for $(n+1) = 4$,

$$\mathscr{A}(\{n+1\}, p) = 2c\, x_{12}^{n} \quad . \tag{2.15}$$

The notation for amplitude graphs will be generalized to N-body graphs in the next section. For now, we only note that the topological index of an amplitude graph will always be defined by counting the dotted interaction line (arising from the last application of V) in the same way as all of the wiggly exchange lines. Thus, for example, the amplitude graph in Fig. 6(a) has the same topological index as the wave function graph in Fig. 3(a). Now, (2.15) may be written

$$\mathscr{A}(\{n+1\}, p) = 2x_{12}^{n+1}(k_1 - k_2)\mathscr{S}_p(k_1 - p_1)\left(\frac{-i}{k_1 - p_1 - i\epsilon}\right) . \tag{2.16}$$

Noting that $\mathscr{S}_p(p_1 - p_2) = 0$ we can write

$$\mathscr{A}(\{n+1\}\ p) = 2x_{12}^{n+1}\mathscr{S}_p\left[(k_1 - k_2) + (p_1 - p_2)\right](k_1 - p_1)\left(\frac{-i}{k_1 - p_1 - i\epsilon}\right)$$

$$= \mathscr{S}_p\left[(k_1 + p_1)(k_1 - p_1) - (k_2 + p_2)(p_2 - k_2)\right]\mathscr{G}(\{n+1\}, p)$$

$$= (\omega_k - \omega_p)\mathscr{G}(\{n+1\}, p) \quad . \tag{2.17}$$

Now, when G_0 is applied to the $(n+1)$th order amplitude graph, it gives an energy denominator which cancels the first factor in (2.17), leaving the factorized wave function graph $\mathscr{G}(\{n+1\})$. This demonstrates by induction that the factorized graphs are equivalent to ordinary perturbation theory for two-body scattering. The procedure followed here will be generalized to the N-body scattering problem in the next section. It is helpful in this regard to associate the energy differences $\left(k_1^2 - p_1^2\right)$ and $\left(k_2^2 - p_2^2\right)$ in (2.17) with numbered particle lines 1 and 2 respectively.

III. N-BODY SCATTERING: REDUCTION OF PERTURBATION THEORY TO FACTORIZED GRAPHS

Having developed some techniques for classifying and manipulating factorized graphs, we can now describe the general inductive procedure by which the perturbation series (2.1) for the N-body wave function can be reduced to a sum of factorized graphs. The treatment is similar to that of the two-body problem discussed in Section II. We assume that the factorization has been carried out on the nth order wave function graphs and consider the construction of the (n + 1)th order graphs by attaching one more vertex and one more energy denominator (successive application of V and G_0). The reduction of the (n + 1)th order graphs is facilitated by generalizing a trivial observation about the two-body system. In that case, we note that the amplitude graph $\mathscr{A}(\{n+1\})$ evolved, by the application of G_0, into the wave function graph of the same topology, i.e. $\mathscr{G}(\{n+1\})$. (Recall that, by definition, the topological index of an amplitude graph is found by ignoring the distinction between the dotted line and the wiggly lines.) In the N-body system, the situation is complicated by the fact that a factorized amplitude graph is not completely determined by its topological index, since this quantity does not specify which pair of particle lines is contracted by the dotted line vertex. For an amplitude graph with topology $\{m\}$, this contraction may occur between any of the pairs (i, j) which have $m_{ij} \neq 0$. Thus, there are $\hat{m}$ distinct amplitude graphs with topology $\{m\}$, where $\hat{m}$ is calculated from $\{m\}$ via (2.8) and (2.12). It will be found that

these $\hat{m}$ amplitude graphs combine very nicely and evolve, under the application of G_0, into the single wave function graph with topology $\{m\}$. In order to show this we must discuss some properties of factorized amplitude graphs.

The amplitude graph with topological index $\{m\}$ in which particle lines i and j are contracted by the dotted line at the top of the graph will be denoted $\mathscr{A}_{ij}(\{m\})$. For example, the graph in Fig. 6(a) is $\mathscr{A}_{12}(\{3, 1, 0, 0, 2, 2\})$. An amplitude graph is computed by the rules (2.5) along with a factor 2c for the dotted line vertex. Again it is helpful to write the graph as the product of a skeleton graph and a dressing function. The dressing function of an amplitude graph is conveniently written in terms of the dressing function (2.11) for the wave function graph of the same topology. Specifically, the dressing function for the amplitude graph $\mathscr{A}_{ij}(\{m\}, p)$ is defined to be

$$(-i)(k_i - k_j)\mathscr{D}(\{m\}) \quad . \tag{3.1}$$

The remaining factors in the graph, coming from momentum denominators and loop integrations, are included in the skeleton. A technicality involving factors of 2 can be elucidated by considering two cases separately, $m_{ij} = 1$ and $m_{ij} > 1$. For $m_{ij} = 1$, the dotted line is the only interaction which connects particle lines i and j. The reduction of the skeleton graph to one with topology $\{\hat{m}\}$ (defined as in (2.8)) can be achieved by repeated use of (2.9) or Fig. 4. In this case, the factor $2^{\hat{m}}$ contained in (2.18) appears

as $2^{\hat{m}-1}$ from rule (2.5d) and 2 from the dotted line vertex factor 2c. On the other hand, if $m_{ij} > 1$, there is already a factor of $2^{\hat{m}}$ from rule (2.5d) and there might seem to be an extra factor of 2 in this case. This factor is in fact cancelled during the reduction of the skeleton to one with topology $\{\hat{m}\}$. The removal of the last wiggly line connecting i and j involves a loop integral with only one momentum denominator. The divergence of this integral is an artifact which is removed by an explicit symmetrization of the intermediate state momenta, producing a factor of 1/2. Thus the skeleton of an amplitude graph $\mathscr{A}_{ij}(\{m\})$ is calculated by removing all wiggly lines connecting i and j (leaving only the dotted line), removing all but one wiggly line connecting any other pair, and computing this reduced graph by rules (2.5a and c). For example, the skeleton of Fig. 6(a) reduces to Fig. 6(b). The dotted line in such a reduced skeleton incurs no factors at all except insofar as it may complete a closed loop.

It can now be seen that the rules for calculating the skeleton of an amplitude graph $\mathscr{A}_{ij}(\{m\}, p)$ which will be denoted $\mathscr{K}_{ij}(\{m\}, p)$, are identical to those for the wave function skeleton $\mathscr{K}(\{m\}, p)$ except that the latter contains an extra factor of $(-i)(q_{ij} - i\epsilon)^{-1}$. Here and elsewhere, q_{ij} is the momentum transferred across the interaction line connecting particle lines i and j in a reduced skeleton graph. This exchange may or may not be part of a closed loop. In the following, we will be combining the $\hat{m}$ amplitude graphs $\mathscr{A}_{ij}(\{m\}, p)$. Their skeletons all have an identical topology $\{\hat{m}\}$. We choose to route the loop momenta in each of these

skeletons in a topologically identical way. The graphs can then be combined before the loop integrals are carried out, treating the momentum passing through any exchange line as the same in each graph (i.e. it is the same function of initial, final, and loop momenta).

It will be convenient to define certain sets associated with a particular topology $\{\hat{m}\}$. Let $\mathscr{C}(\{\hat{m}\})$ be the set of all pairs of integers (i, j) such that $i < j \leq N$ and $\hat{m}_{ij} \neq 0$.

$$\mathscr{C}(\{\hat{m}\}) = \left\{(i, j) \,\middle|\, i < j \leq N \text{ and } \hat{m}_{ij} \neq 0\right\} . \tag{3.2}$$

$\mathscr{C}(\{\hat{m}\})$ contains $\hat{m}$ pairs, each one denoting a particular exchange line in the reduced skeleton $\mathscr{K}(\{\hat{m}\})$ or $\mathscr{K}_{ij}(\{\hat{m}\})$. We can also associate two sets of single integers, $\phi_j^{>}(\{\hat{m}\})$ and $\phi_j^{<}(\{\hat{m}\})$, with each particle line j,

$$\phi_j^{>}(\{\hat{m}\}) = \left\{\ell \mid \ell > j \text{ and } \hat{m}_{j\ell} \neq 0\right\} \tag{3.3}$$

$$\phi_j^{<}(\{\hat{m}\}) = \left\{i \mid i < j \text{ and } \hat{m}_{ij} \neq 0\right\} . \tag{3.4}$$

In the wave function skeleton $\mathscr{K}(\{\hat{m}\})$, $\phi_j^{<}$ and $\phi_j^{>}$ enumerate, respectively, all those exchange lines which enter and all those which leave particle line j. This is depicted in Fig. 7. The sum of all amplitude graphs with topology $\{m\}$ can be written

$$\sum_{(i,j) \in \mathscr{C}(\{\hat{m}\})} \mathscr{A}_{ij}(\{m\}, p) = -i\mathscr{D}(\{m\}) \sum_{(i,j) \in \mathscr{C}(\{\hat{m}\})} (k_i - k_j)\mathscr{K}_{ij}(\{\hat{m}\}, p) \tag{3.5}$$

using (3.1). The momenta p_i and p_j emerge from the dotted line vertex at the top of the graph $\mathscr{K}_{ij}(\{m\}, p)$. The latter is therefore symmetric under $p_1 \leftrightarrow p_2$, allowing us to write

$$\mathscr{S}_p \sum_{(i,\,j)\,\in\,\mathscr{C}} \mathscr{A}_{ij}(\{m\}, p) = -i\mathscr{D}(\{m\})\mathscr{S}_p \sum_{(i,\,j)\,\in\,\mathscr{C}} \left[(k_i + p_i) - (k_j + p_j)\right]\mathscr{K}_{ij}(\{\hat{m}\}, p) \quad . \tag{3.6}$$

With the previously defined set notation, this becomes

$$\begin{aligned}\mathscr{S}_p \sum_{(i,\,j)\,\in\,\mathscr{C}} \mathscr{A}_{ij}(\{m\}, p) &= -i\mathscr{D}(\{m\})\mathscr{S}_p \left\{ \sum_{i=1}^{N} \sum_{j\,\in\,\Phi_i}^{>} (k_i + p_i)\mathscr{K}_{ij}(\{\hat{m}\}, p) \right. \\ &\qquad \left. - \sum_{j=1}^{N} \sum_{i\,\in\,\Phi_j}^{<} (k_j + p_j)\mathscr{K}_{ij}(\{\hat{m}\}, p) \right\} \qquad (3.7) \\ &= -i\mathscr{D}(\{m\})\,\mathscr{S}_p \sum_{j=1}^{N} (k_j + p_j) \left\{ \sum_{\ell\,\in\,\Phi_j}^{>} \mathscr{K}_{j\ell}(\{\hat{m}\}, p) - \sum_{i\,\in\,\Phi_j}^{<} \mathscr{K}_{ij}(\{\hat{m}\}, p) \right\} \quad .\end{aligned}$$

The sum inside the brackets in Eq. (3.7), taken prior to the loop integrals as previously described, involves a simple sum of exchange momenta connecting to particle line j, viz.

$$\sum_{\ell\,\in\,\Phi_j}^{>} q_{j\ell} - \sum_{i\,\in\,\Phi_j}^{<} q_{ij} = k_j - p_j \quad . \tag{3.8}$$

Using this, it can be shown that

$$\sum_{\ell \in \Phi_j}{}_{>} \mathscr{K}_{j\ell}(\{\hat{m}\}, p) - \sum_{i \in \Phi_j}{}_{<} \mathscr{K}_{ij}(\{\hat{m}\}, p) = i(k_j - p_j)\mathscr{K}(\{\hat{m}\}, p) \quad . \tag{3.9}$$

Eq. (3.7) thus becomes

$$\mathscr{S}_p \sum_{(i,\, j) \in \mathscr{C}} \mathscr{A}_{ij}(\{m\}, p) = \sum_{j=1}^{N} (k_j^2 - p_j^2)\mathscr{S}_p \mathscr{G}(\{m\}, p) \quad . \tag{3.10}$$

The first factor cancels the final energy denominator, showing that the sum of topologically similar amplitude graphs evolves into the wave function graph with the same topology. Applying this procedure to all topologies $\{m\}$ establishes to order $m = n + 1$ the equivalence of factorized graphs and ordinary perturbation theory.

IV. WAVE FUNCTIONS, BILLIARD BALLS, AND BETHE'S HYPOTHESIS

The reduction of perturbation theory to factorized graphs provides a remarkable simplification in the graphical representation of many-body in-state wave functions. In this section we will examine these wave functions in more detail and establish the connection with Bethe's hypothesis. One can go a long way toward understanding the nature of the N-body wave functions and their emergence as a sum of dressed skeletons in perturbation theory by considering the analogous description of a system of idealized pointlike classical particles (billiard balls) moving in one dimension. The state of such a system is specified by giving the coordinates $(x_1, \ldots, x_N)$ and velocities $(v_1, \ldots, v_N)$ of all the particles. If all the particles are identical, then any state can be described by coordinates x_i chosen such that

$$x_1 > x_2 > \ldots > x_N \quad . \tag{4.1}$$

At $t = -\infty$ an in-state is a collection of widely separated particles with velocities

$$v_1 < v_2 < \ldots < v_N \quad . \tag{4.2}$$

The time development of this system up to $t = 0$ consists of some number of two-body collisions interspersed by free motion. In each collision, energy and momentum conservation dictate that the two particles emerge with

the same pair of velocities they had before the collision. Thus at $t = 0$, the system still contains the same N velocities it began with. This allows us to form a correspondence between the possible states of the classical system at $t = 0$ and the elements of the permutation group S_N. If the particles are located at $(x_1, x_2, \ldots, x_N)$, chosen to satisfy (4.1), the N! possible velocity arrangements are $(v_{P_1}, v_{P_2}, \ldots, v_{P_N})$, where $(P_1, P_2, \ldots, P_N)$ is some permutation of (12 ... N). For some purposes it is more convenient to identify such a state with the permutation $Q \equiv P^{-1}$ by listing the velocities in their natural order $(v_1, v_2, \ldots, v_N)$ and then specifying their arrangement in coordinate space $(x_{Q_1}, x_{Q_2}, \ldots, x_{Q_N})$. The time evolution of the system from $t = -\infty$ to $t = 0$ can be described by labelling each two-body collision which takes place in that interval according to the pair of velocities (v_i, v_j) which participate. Any particular pair of velocities (v_i, v_j) can collide at most once. Therefore, the time evolution can be characterized by a collection of $N(N-1)/2$ numbers $\{\hat{n}_{ij}\}$, where $\hat{n}_{ij} = 1$ if the collision (v_i, v_j) took place and $\hat{n}_{ij} = 0$ otherwise. This is clearly the classical analog of the topological index of a reduced skeleton graph. The identification of a particle by its velocity v_i corresponds to the numbering of a particle line in a factorized graph according to its "pseudomomentum" k_i. The distinction between the pseudomomentum and the true momentum carried by the line and the appearance of momentum denominators in a factorized graph reflect the restrictions of quantum mechanical uncertainty.

Further pursuit of this classical analogy serves to introduce the remainder of this section in which we trace the connection between the factorized skeleton graph expansion of the N-body wave function and the form given by Bethe's hypothesis. Consider the possible states of the classical system at $t = 0$ which can arise from a given time evolution $\{\hat{n}\}$. The states at $t = 0$ are classified, according to the previous discussion, by a velocity permutation P, or equivalently, by a coordinate permutation $Q = P^{-1}$. We allow the possibility that two particles may pass through each other without interacting. Thus, a time evolution with no interactions, $\hat{n}_{ij} = 0$ for all (i, j), can give rise to any of the N! possible arrangements at $t = 0$. On the other hand, a collision (v_i, v_j) with $v_i < v_j$ at some time $t < 0$ restricts the possibilities at all subsequent times to those which have $Q_i > Q_j$ (i.e., by (4.1), $x_{Q_i} < x_{Q_j}$). Thus, the possible states at $t = 0$ which can arise from a particular time evolution $\{\hat{n}\}$ are described by coordinate permutations Q which satisfy $Q_i > Q_j$ for all (i, j) such that $\hat{n}_{ij} \neq 0$.

With this classical motion in mind we return to the quantum mechanical system and study the skeleton expansion of the in-state wave function

$$\langle p \left| \Psi^{(+)}(k) \right\rangle = (2\pi)\,\delta(\Sigma_N(p) - \Sigma_N(k)) \sum_{\{\hat{n}\}} \tilde{\mathscr{D}}(\{\hat{n}\})\,\mathscr{K}(\{\hat{n}\}, p) \quad . \tag{4.3}$$

Here and in the following, we use the abbreviation

$$\sum\nolimits_{\ell}(k) \equiv \sum_{i=1}^{\ell} k_i \quad . \tag{4.4}$$

In Eq. (4.3), $\tilde{\mathscr{D}}(\{\hat{n}\})$ is the full dressing function of the skeleton $\mathscr{K}(\{\hat{n}\})$, which is calculated by summing $\mathscr{D}(\{n\})$ over all topologies $\{n\}$ that reduce to $\{\hat{n}\}$ by (2.8). This gives

$$\tilde{\mathscr{D}}(\{\hat{n}\}) = 2^{\hat{n}} \prod_{(i,j) \in \mathscr{C}(\{\hat{n}\})} \left(\sum_{\ell=1}^{\infty} x_{ij}^{\ell} \right) = \prod_{(i,j) \in \mathscr{C}(\{\hat{n}\})} \tau_{ij} \tag{4.5}$$

where

$$\tau_{ij} = \frac{2x_{ij}}{1 - x_{ij}} = e^{i\theta_{ij}} - 1 \quad . \tag{4.6}$$

We use $\theta_{ij} = 2 \tan^{-1}\left[c/(k_i - k_j)\right]$ to denote the two-body phase shift. The connection between Bethe's hypothesis and the skeleton expansion (4.3) can be made clear by introducing a simple concept of formal set theory, that of a power set. For any set $\mathscr{E}$, the power set $\mathscr{P}(\mathscr{E})$ is defined as the set of all subsets of $\mathscr{E}$. Symbolically,

$$\mathscr{P}(\mathscr{E}) = \left\{ X \,|\, X \subset \mathscr{E} \right\} . \tag{4.7}$$

Thus, for example, if $\mathscr{E}$ is a set of two elements $\mathscr{E} = \{a, b\}$, the power set $\mathscr{P}(\mathscr{E})$ contains four elements ϕ (empty), $\{a\}$, $\{b\}$, and $\{a, b\}$. In general, if $\mathscr{E}$ has n elements, $\mathscr{P}(\mathscr{E})$ has 2^n elements. We will now show that the set of all distinct N-body skeleton graphs, or equivalently, the set of reduced topological indices $\{\hat{n}\}$, has the structure of a power set. Let us define the set containing N(N - 1)/2 integer pairs

$$\mathscr{E}_N = \left\{(i, j) \middle| i < j \leq N\right\} \quad . \tag{4.8}$$

It is seen that for any N-body reduced topology $\{\hat{n}\}$, $\mathscr{C}(\{\hat{n}\}) \subset \mathscr{E}_N$, where $\mathscr{C}(\{\hat{n}\})$ is defined by Eq. (3.2). Thus, each $\mathscr{C}(\{\hat{n}\})$ is an element of the power set $\mathscr{P}(\mathscr{E}_N)$. Conversely, every element of $\mathscr{P}(\mathscr{E}_N)$ is equal to some $\mathscr{C}(\{\hat{n}\})$ where $\{\hat{n}\}$ describes some N-body skeleton. Since the correspondence between reduced topologies $\{\hat{n}\}$ and sets $\mathscr{C}(\{\hat{n}\})$ is one-to-one, we can denote a reduced topology by the corresponding element $\mathscr{C}$ of the power set $\mathscr{P}(\mathscr{E}_N)$ (e.g. the non-interacting skeleton corresponds to the empty set, and so forth). It will in fact be convenient to regard the skeleton expansion (4.3) as a sum over elements of $\mathscr{P}(\mathscr{E}_N)$,

$$\langle p \left| \Psi^{(+)}(k) \right\rangle = (2\pi)\delta(\Sigma_N(p) - \Sigma_N(k)) \sum_{\mathscr{C} \in \mathscr{P}(\mathscr{E}_N)} \tilde{\mathscr{D}}(\mathscr{C}) \mathscr{K}(\mathscr{C}, p) \quad . \tag{4.9}$$

The manipulation of (4.9) into the form of the wave function given by Bethe's hypothesis hinges on a fundamental decomposition property of skeleton graphs. Appealing to our classical billiard ball system for guidance, we are led to define, for any pair $(i, j) \in \mathscr{E}_N$, a set which contains half the elements of the permutation group S_N

$$\pi(i, j) = \left\{P \in S_N \middle| (P^{-1})_i > (P^{-1})_j\right\} \quad . \tag{4.10}$$

In the previous classical discussion, $\pi(i, j)$ would be just the set of velocity permutations at $t = 0$ which can be reached by a time development consisting of a single collision between velocities v_i and v_j. To discuss classical time developments involving more than one collision (or quantum mechanical skeletons involving more than one exchange) we must consider the intersection of $\pi(i, j)$'s over a set of pairs $\mathscr{C}$,

$$\pi(\mathscr{C}) = \bigcap_{(i, j) \in \mathscr{C}} \pi(i, j) \quad . \tag{4.11}$$

An N-particle plane wave with momenta k_i can be decomposed into N! pieces corresponding to the possible spatial orderings of the k_i's by defining the "ordered plane waves"

$$\Phi(P; p) = N! \, \mathscr{S}_p (2\pi)\delta(\Sigma_N(p) - \Sigma_N(k)) \prod_{\ell = 1}^{N-1} \left[\frac{-i}{\Sigma_\ell(p) - \Sigma_\ell(Pk) - i\epsilon} \right] \tag{4.12}$$

where

$$\Sigma_\ell(Pk) = \sum_{i = 1}^{\ell} k_{P_i} \quad . \tag{4.13}$$

The functions (4.12) are the N-body generalization of Eq. (4.8) of I. The fact that these functions are the pieces of a plane wave is demonstrated by the identity

$$\sum_{P \in S_N} \Phi(P; p) = N! \, (2\pi)^N \mathscr{S}_p \prod_{i = 1}^{N} \delta(p_i - k_i) = \langle p | k \rangle \quad . \tag{4.14}$$

The decomposition of a skeleton graph $\mathscr{K}(\mathscr{C})$ expresses it as a sum of ordered plane waves over the set of permutations $\pi(\mathscr{C})$,

$$(2\pi)\delta(\Sigma_N(p) - \Sigma_N(k))\mathscr{K}(\mathscr{C}; p) = \sum_{P \in \pi(\mathscr{C})} \Phi(P;p) \quad . \tag{4.15}$$

This is exactly the decomposition one might have guessed from the preceeding classical arguments. The proof of (4.15) is most easily carried out graphically by introducing a skeleton graph-like representation of the functions $\Phi(P)$. Attaching this graphical $\Phi(P)$ to the top of a skeleton graph and summing over permutations leaves the skeleton graph unchanged, by (4.14). When loop integrations are carried out, each term in this sum reduces to either $\Phi(P)$ if $P \in \pi(\mathscr{C})$ or to zero if $P \notin \pi(\mathscr{C})$, giving (4.15).

Using (4.5) and (4.15), the expansion (4.9) becomes

$$\langle p | \Psi^{(+)}(k) \rangle = \sum_{\mathscr{C} \in \mathscr{G}(\mathscr{E}_N)} \left[\sum_{P \in \pi(\mathscr{C})} \Phi(P; p) \prod_{(i,j) \in \mathscr{C}} \tau_{ij} \right] \quad . \tag{4.16}$$

The order of summation in (4.16), i.e. a sum over permutations contained in each skeleton followed by a sum over all skeletons, is characteristic of the graphical perturbative approach to this system. Bethe's hypothesis comes about by interchanging this order of summation. To do this, we associate a certain subset of $\mathscr{E}_N$ with each permutation,

$$\mathscr{A}(P) = \left\{ (i,j) \in \mathscr{E}_N \,\middle|\, (P^{-1})_i > (P^{-1})_j \right\} \quad . \tag{4.17}$$

In the classical analogy, $\mathscr{X}(P)$ can be thought of as the set of all collisions (v_i, v_j) which can occur in the system at $t < 0$ without precluding a state with velocity permutation P at $t = 0$. Note the similarity between $\mathscr{X}(P)$, which maps elements of S_N onto subsets of $\mathscr{E}_N$, and $\pi(i, j)$ which maps elements of $\mathscr{E}_N$ onto subsets of S_N. We now observe that the statement $P \in \pi(\mathscr{C})$ is valid if and only if $\mathscr{C} \subset \mathscr{X}(P)$. Physically this is just the trivial assertion that if a certain time development described by a set of collisions $\mathscr{C}$ can give rise to a certain velocity permutation P then $\mathscr{C}$ contains no collisions which preclude P, and conversely. This allows us to invert the order of summation in (4.16),

$$\langle p | \Psi^{(+)}(k) \rangle = \sum_{P \in S_N} \Phi(P; p) \left[\sum_{\mathscr{C} \in \mathscr{P}(\mathscr{X}(p))} \prod_{(i, j) \in \mathscr{C}} \tau_{ij} \right]. \qquad (4.18)$$

We see that, just as the full set of N-body skeletons can be identified with the power set of $\mathscr{E}_N$, the set of all skeletons which contribute to a particular ordered plane wave $\Phi(P)$ can be identified with the power set of a subset of $\mathscr{E}_N$, namely, with $\mathscr{P}(\mathscr{X}(P))$. This is intimately connected with the appearance of simple additive phase shifts in Bethe's hypothesis, since

$$\sum_{\mathscr{C} \in \mathscr{P}(\mathscr{X}(p))} \left[\prod_{(i, j) \in \mathscr{C}} \tau_{ij} \right] = \prod_{(i, j) \in \mathscr{X}(P)} (1 + \tau_{ij}). \qquad (4.19)$$

With this, the wave function becomes

$$\langle p \mid \Psi^{(+)}(k) \rangle = \sum_{P \in S_N} \Phi(P; p) \prod_{(i,j) \in \mathscr{L}(P)} e^{i\theta_{ij}} . \qquad (4.20)$$

An inspection of the set $\mathscr{L}(P)$ reveals that (4.17) is equivalent to the familiar algorithm for determining the phase shifts in Bethe's hypothesis.

V. SCATTERING THEORY OF THE SECOND VIRIAL COEFFICIENT

The simplicity achieved in the description of many-body scattering processes by the introduction of factorized graphs encourages one to seek a similar understanding of finite density systems. The present section sketches some initial efforts in that direction. A fuller discussion of this subject will be given in a subsequent publication. Of course, the relationship between two-body scattering and the second virial coefficient is well understood,[12] and the result obtained here is nothing new. This calculation does show, however, that by using factorized graphs, one can avoid the usual procedure of putting the system in a box and imposing periodic boundary conditions to determine the density of states. In our approach the (volume) $\rightarrow \infty$ limit is replaced by the $i\epsilon \rightarrow 0$ limit of scattering theory. This limit requires some delicacy due to the forward singularities of the matrix element involved.[13] It is interesting that the derivative which acts on the phase shift in the familiar expression for the two-body density of states arises, in this calculation, as the manifestation of a forward singularity. It seems likely that the conversion of forward singularities

into momentum derivatives will also be important in the theory of higher virial coefficients for this model. The role played by unitarity of the Moeller wave operators may also be of more general interest. The method used here to relate partition functions to operator scattering theory is inspired by the work of Dashen et al.,[11] and earlier work by Goldberger,[10] though it differs in detail enough to warrant some discussion.

Following Goldberger, we write the N-body partition function as a contour integral in the complex energy plane,

$$Q_N = \mathrm{Tr}_N(e^{-\beta H}) = \int_C \frac{dE}{2\pi i} e^{-\beta E} \mathrm{Tr}_N G(E) \tag{5.1}$$

where $G(E) = (E - H)^{-1}$ and Tr_N indicates a trace over the N-particle sector of the Hilbert space. The contour in (5.1) goes from $+\infty$ above the real axis, to the left of all singularities of the trace, and back to $+\infty$ below the real axis. Only repulsive potentials ($c > 0$) are considered, and hence all discontinuities are at $\mathrm{Re}\, E \geq 0$. Letting the contour close around the real axis, (5.1) becomes

$$\begin{aligned} Q_N &= \int_{0+i\epsilon}^{\infty+i\epsilon} \frac{dE}{2\pi i} e^{-\beta E} \mathrm{Tr}_N\left[G^+(E) - G(E)\right] \\ &= \int_{0+i\epsilon}^{\infty+i\epsilon} dE\ e^{-\beta E} \mathrm{Tr}_N\left[\delta(E - H_o)\Omega^+(E)\Omega(E)\right] . \end{aligned} \tag{5.2}$$

The operators in (5.2) are defined by

$$(2\pi i)\delta(E - H_0) = G_0^{+}(E) - G_0(E) \tag{5.3}$$

$$\Omega(E) = \sum_{n=0}^{\infty} \left[G_0(E)V\right]^n \quad , \tag{5.4}$$

with $G_0^{+}(E) = G_0(E^{*})$. The last expression in (5.2) is obtained by expanding G and G^{+} in perturbation theory and using the cyclic property of the trace. By virtue of the perturbation expansion of (5.2), the partition function Q_N may be realized as a sum of "vacuum" diagrams (forward matrix element diagrams with initial particle lines contracted with final particle lines in all N! possible ways). The equation of state of a finite density system is most easily constructed from Q_{Nc} = sum of connected vacuum diagrams. Note that the connectedness of a vacuum diagram is not necessarily the same as that of the matrix element from which it came, since the contraction of initial and final lines can convert a disconnected matrix element diagram into a connected vacuum diagram (e.g. $Q_{Nc} \neq 0$ even for an ideal gas). The thermodynamics of a system is obtained by writing the log of the grand partition function $\mathcal{Q}$ as a sum of connected diagrams,

$$\log \mathcal{Q} = \sum_{N=1}^{\infty} z^N Q_{Nc} \tag{5.5}$$

where z = fugacity.

Now we consider specifically the case N = 2 and write

$$Q_{2c} = \lim_{\epsilon \to 0} \frac{1}{2!} \int \frac{dk_1}{2\pi} \frac{dk_2}{2\pi} e^{-\beta(k_1^2 + k_2^2)} \langle k_1 k_2 \mid \Omega^+(\omega_k + i\epsilon)\Omega(\omega_k + i\epsilon) \mid k_1 k_2 \rangle_c \quad (5.6)$$

Expressing the matrix element in (5.6) in terms of factorized graphs, we see that the part of Q_{2c} which depends on the interaction is given by the two contractions of the dressed skeleton $\{1\}$, Fig. 8 and Fig. 9. The delicacy of the $\epsilon \to 0$ limit is due to the diagram in Fig. 8. Since the momentum transferred across the exchange line is forced to vanish, the skeleton is proportional to $1/(i\epsilon)$. However, the dressing function for Fig. 8 is $2(\tau_{12} + \tau_{12}^* + \tau_{12}\tau_{12}^*) = 0$ and the dressed graph therefore vanishes. A calculation of Q_{2c} using Fig. 9 only can be carried out and gives the correct answer. Here we take an alternative approach which is more closely related to the original Beth-Uhlenbeck procedure.[12] In the limit $\epsilon \to 0$, $\Omega(\omega_k + i\epsilon)$ becomes the Moeller wave operator $U(0, -\infty)$ (when acting on a state of energy ω_k). Thus, by the unitarity of $U(0, -\infty)$,

$$\lim_{\epsilon \to 0} \langle k_1' k_2' \mid \Omega^+(\omega_{k'} + i\epsilon)\Omega(\omega_k + i\epsilon) \mid k_1 k_2 \rangle = \langle k_1' k_2' \mid k_1 k_2 \rangle \quad (5.7)$$

when $k_i' \neq k_i$. This allows us to write

$$Q_{2c} - Q_{2c}^{(0)} = \frac{1}{2!} \int \frac{dk_1}{2\pi} \frac{dk_2}{2\pi} e^{-\beta(k_1^2 + k_2^2)} \left[\lim_{\epsilon \to 0} \lim_{k_i' \to k_i} - \lim_{k_i' \to k_i} \lim_{\epsilon \to 0} \right]$$

$$\times \langle k_1' k_2' \mid \Omega^+(\omega_k + i\epsilon)\Omega(\omega_k + i\epsilon) \mid k_1 k_2 \rangle \quad (5.8)$$

where $Q_2^{(0)}$ is the partition function for free particles. This matrix element is again computed from the skeletons in Fig. 8(a) and Fig. 9(a). The graph in Fig. 9(a) is perfectly regular in the forward limit even when $\epsilon \to 0$. The $k_i' \to k_i$ and $\epsilon \to 0$ limits of this graph commute and it gives no contribution to (5.8). On the other hand, Fig. 8(a) develops a forward singularity in the $\epsilon \to 0$ limit. Its dressing function is

$$2(\tau_{12} + \tau^*_{1'2'} + \tau_{12}\tau^*_{1'2'}) = 2\left[e^{i(\theta_{12} - \theta_{1'2'})} - 1\right]$$

$$\widetilde{k_i' \to k_i}\ 2i\,(k_2' - k_2)\frac{\partial\theta_{12}}{\partial k_1} \quad . \tag{5.9}$$

The skeleton is $(-i)(k_2' - k_2 - i\epsilon)^{-1}$. The commutation of limits in (5.8) thus gives a factor $-2\frac{\partial\theta_{12}}{\partial k_1}$. The phase shift derivative may be written explicitly as

$$\frac{\partial\theta_{12}}{\partial k_1} = \frac{2c}{(k_1 - k_2)^2 + c^2} - 2\pi\,\delta(k_1 - k_2) \quad . \tag{5.8}$$

Equation (5.8) becomes

$$Q_2 - Q_2^{(0)} = -2\pi\,\delta(0)\int \frac{dk_1}{2\pi}\,\frac{dk_2}{2\pi}\,\frac{\partial\theta_{12}}{\partial k_1}\,e^{-\beta(k_1^2 + k_2^2)} \quad , \tag{5.11}$$

which is just a one-dimensional version of the Beth-Uhlenbeck formula.

ACKNOWLEDGMENTS

I would like to express gratitude to Professor C. N. Yang for much advice and encouragement during the course of this work, to Barry McCoy and Craig Tracy for helpful conversations, and to the SUNY Institute for Theoretical Physics, where much of this work was carried out.

REFERENCES

[1] H. B. Thacker, Phys. Rev. D11, 838 (1975).

[2] C. N. Yang, Phys. Rev. Lett. 19, 1312 (1967); Phys. Rev. 168, 1920 (1968).

[3] J. B. McGuire, J. Math. Phys. 5, 622 (1964).

[4] E. Brezin and J. Zinn-Justin, C. R. Acad. Sci. (Paris) B263, 670 (1966).

[5] E. H. Lieb and W. Liniger, Phys. Rev. 130, 1605 (1963); E. H. Lieb, ibid. 130, 1616 (1963).

[6] C. N. Yang and C. P. Yang, J. Math. Phys. 10, 1115 (1969).

[7] C. N. Yang in Critical Phenomena in Alloys, Magnets, and Superconductors, edited by R. E. Mills, E. Ascher, and R.I. Jaffe (McGraw Hill, New York, 1971).

[8] H. A. Bethe, Z. Phys. 71, 205 (1931).

[9] See, for example, K. Huang, Statistical Mechanics (John Wiley and Sons, New York, 1963), Appendix A.

[10] M. L. Goldberger, Phys. Fluids 2, 252 (1959).

[11] R. Dashen, S. Ma, and H. J. Bernstein, Phys. Rev. 187, 345 (1969).

[12] E. Beth and G. E. Uhlenbeck, Physica 4, 915 (1937).

[13] R. Dashen and S. Ma, J. Math. Phys. 11, 1136 (1970); J. Math. Phys. 12, 689 (1971).

FIGURE CAPTIONS

Fig. 1: The basic vertex of ordinary perturbation theory.

Fig. 2: The basic exchange line of factorized graphs.

Fig. 3: (a) An eighth order factorized wave function graph.

(b) The same graphs as Fig. 3(a), after using commutativity of vertices.

(c) The skeleton graph of Fig. 3(a) or 3(b).

Fig. 4: An identity used in the reduction of a skeleton graph.

Fig. 5: (a) The third order factorized two-body wave function graph.

(b) The skeleton graph of Fig. 5(a).

(c) The fourth order two-body amplitude graph.

Fig. 6: (a) An eighth order amplitude graph with the same topology as Fig. 3.

(b) The skeleton graph of Fig. 6(a).

Fig. 7: Numbered particle line j with four exchange lines entering and four exchange lines leaving. In the notation of the text, $i_\kappa \in \phi_j^<$ and $\ell_\kappa \in \phi_j^>$, $\kappa = 1, \ldots, 4$.

Fig. 8: (a) Forward singular skeleton graph for the second virial coefficient.

(b) Vacuum graph obtained by contraction of Fig. 8(a).

Fig. 9: (a) Forward nonsingular skeleton graph for the second virial coefficient.

(b) Vacuum diagram obtained by contraction of Fig. 9(a).

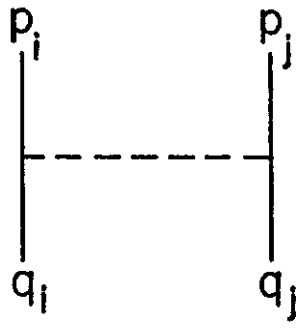

Fig. 1

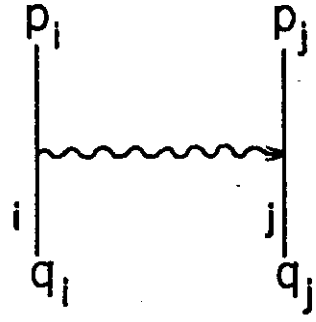

Fig. 2

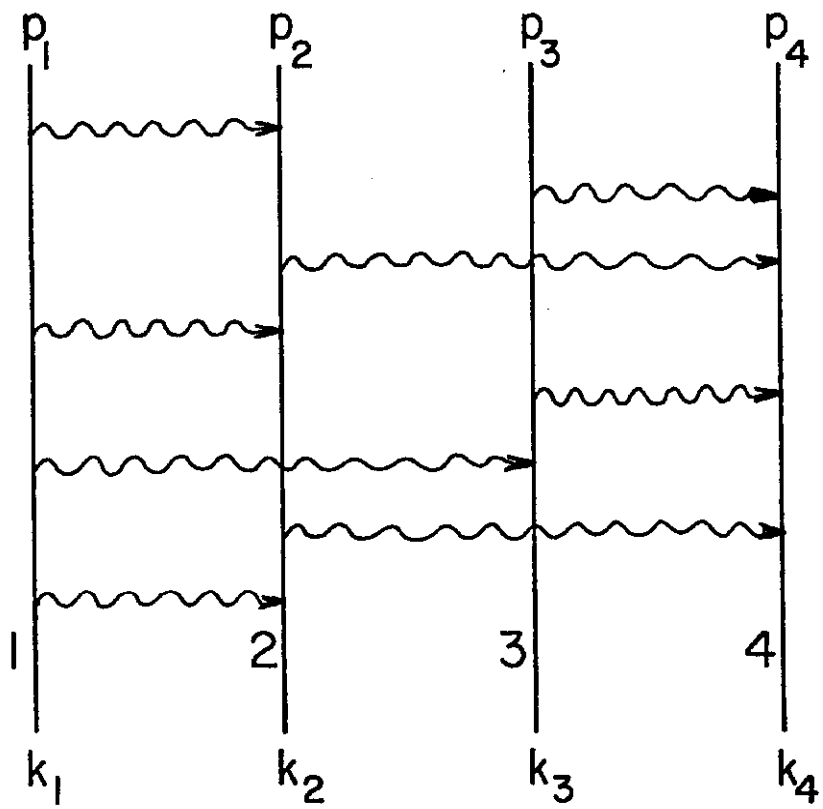

Fig. 3a

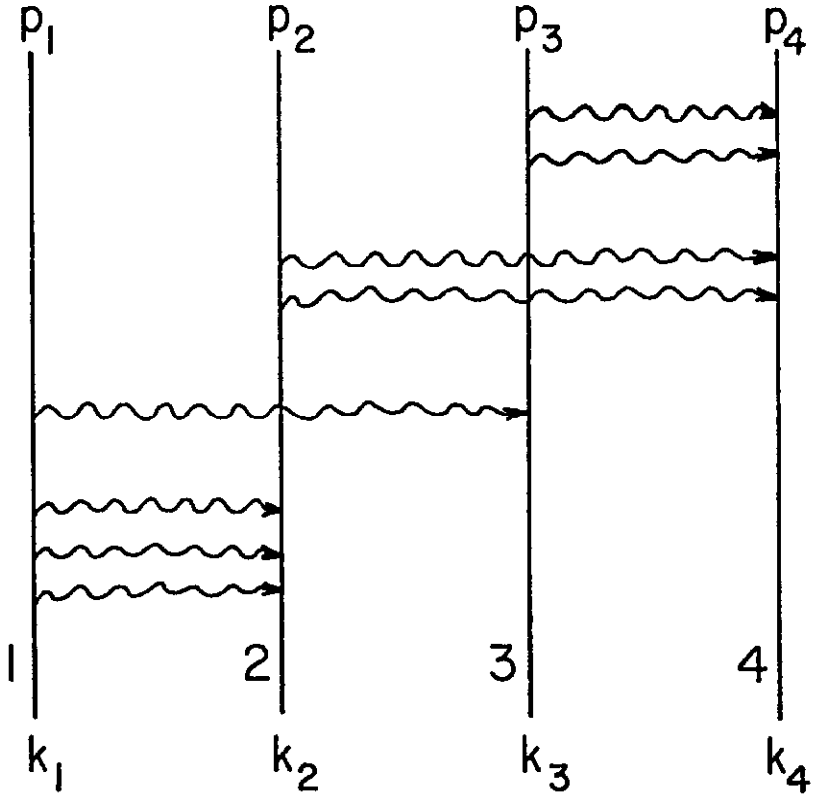

Fig. 3b

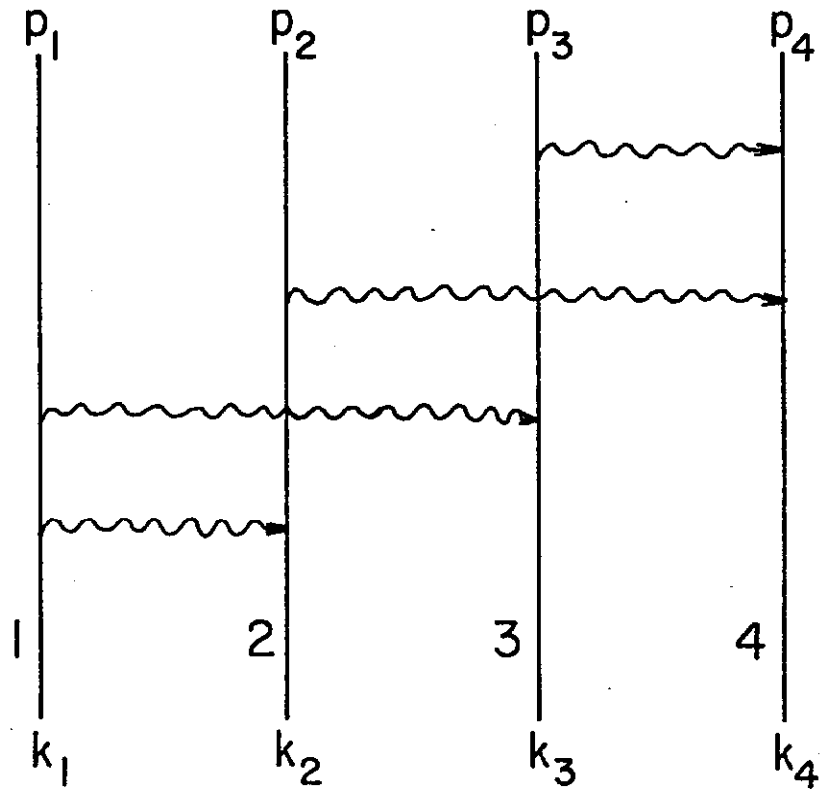

Fig. 3c

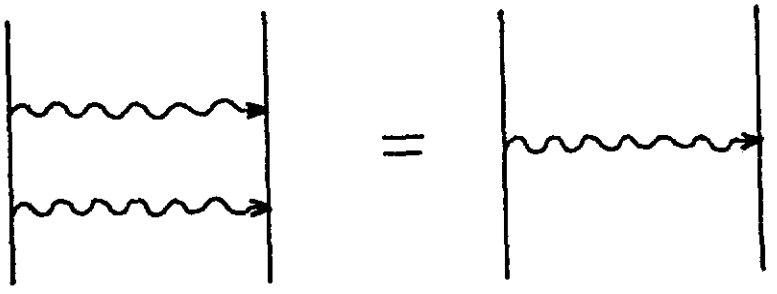

Fig. 4

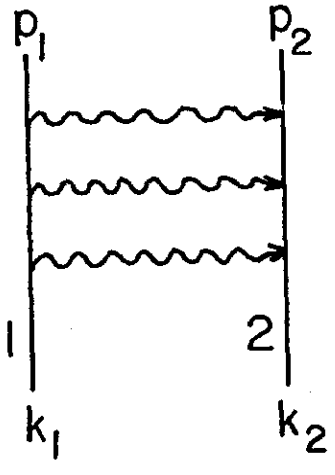

Fig. 5a

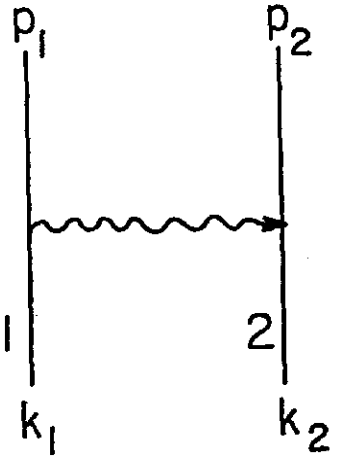

Fig. 5b

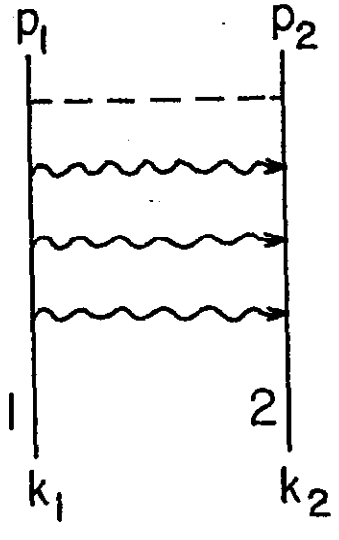

Fig. 5c

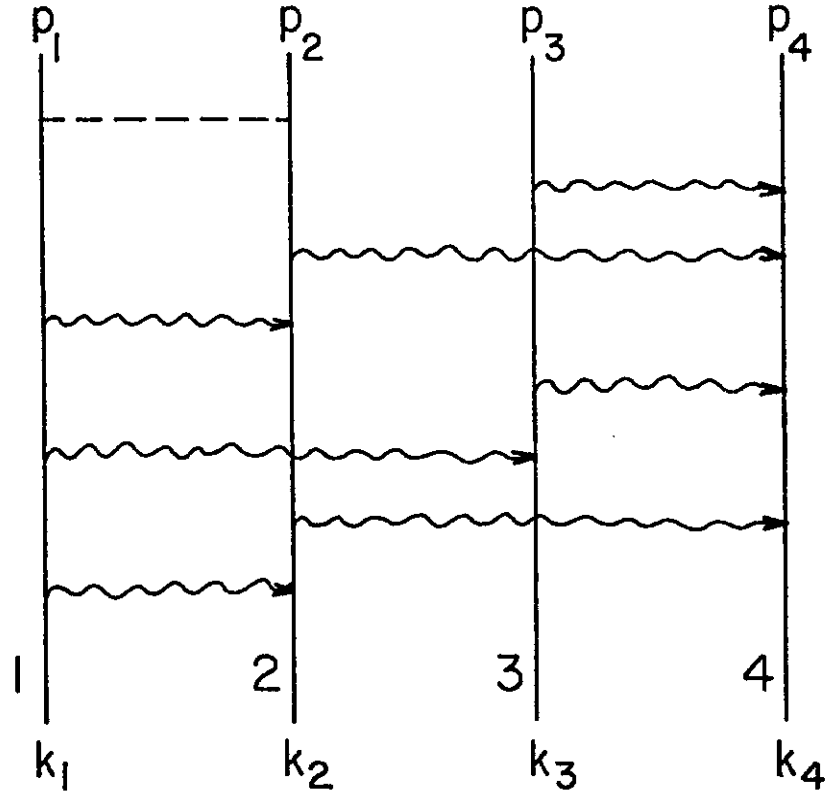

Fig. 6a

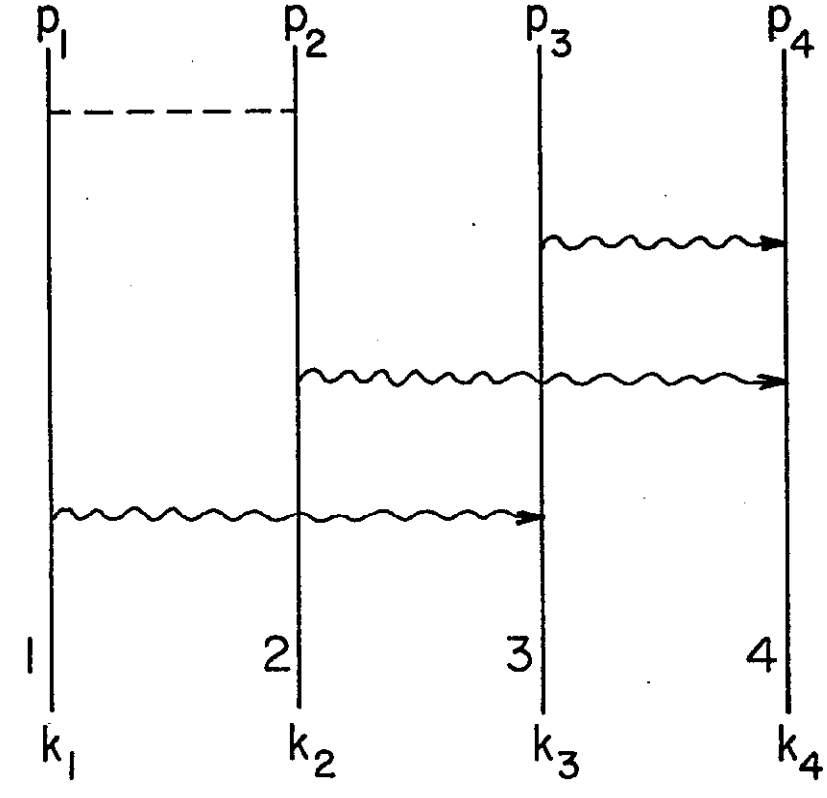

Fig. 6b

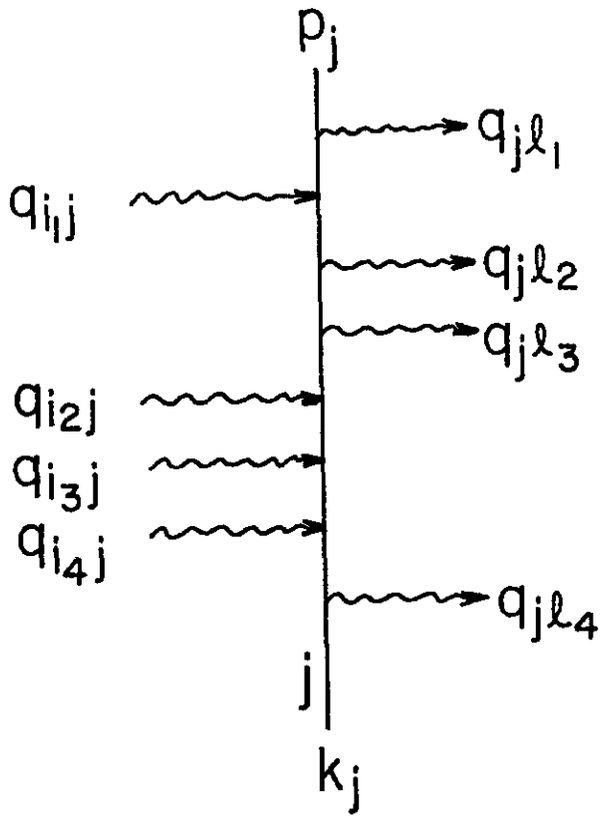

Fig. 7

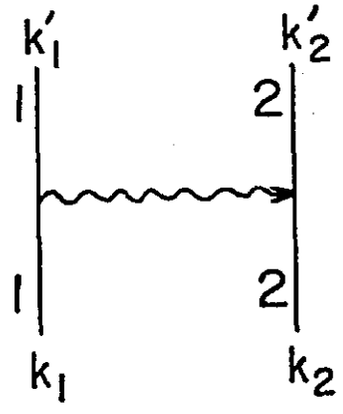

Fig. 8a

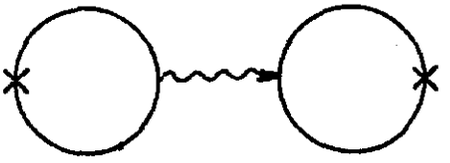

Fig. 8b

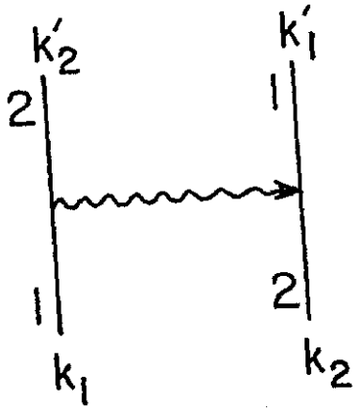

Fig. 9a

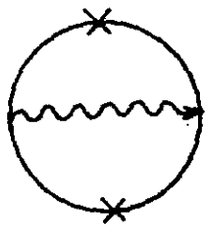

Fig. 9b